Interaction of two axisymmetric bodies falling side by side at moderate Reynolds numbers

Patricia Ern, Nicolas Brosse

Interaction of two axisymmetric bodies falling side by side at moderate Reynolds numbers

Patricia Ern† and Nicolas Brosse

Université de Toulouse, INPT, UPS, IMFT (Institut de Mécanique des Fluides de Toulouse), Allée Camille Soula, F-31400 Toulouse, France

CNRS, IMFT, F-31400 Toulouse, France

We consider the interaction of two identical disks freely falling side by side in a fluid at rest for Reynolds numbers ranging from 100 to 300, corresponding to rectilinear and oscillatory paths. For the three aspect ratios of the disks investigated, we observed that the bodies always repel one another when the horizontal distance between their centres of gravity is less than 4.5 diameters. They never come closer for distances spanning between 4.5 and 6 diameters. Beyond the latter distance, the disks appear indifferent to each other. For both rectilinear and periodic paths, the repulsion effect is weak, leading to an overall horizontal drift lower than 3 % of the vertical displacement. We propose a model for the repulsion coefficient C_r, which decreases with the separation distance between the bodies and is inversely proportional to the aspect ratio of the bodies, C_r thus being stronger for the thicker ones. Furthermore, in the case of the oscillatory paths, we show that the effect of the interaction reduces to the repulsion effect, since the characteristics of the oscillatory motion of each disk appear unaffected by the presence of the companion disk and no synchronization is observed between the paths, nor between the wakes, of the two disks.

Key words: multiphase flow, wakes, vortex interactions

1. Introduction

The problem of the hydrodynamical interaction of two bodies, either free to move in a fluid or fixed in an incident flow, is a question common to biomechanics, multiphase flow and fluid–structure interaction. Primary issues lie in the strength and nature (attractive or repulsive) of the force due to the hydrodynamical interaction between the two objects, and in their relationship with the motion of the bodies, when these are free to move. In this work, we consider the problem of two freely

† Email address for correspondence: ern@imft.fr

falling bodies in the paradigm situation of bodies placed side by side. In the case of two objects placed side by side in an incoming flow or moving side by side at moderate Reynolds numbers, two mechanisms compete to drive their interaction. The first is provided by potential flow analysis and results in an attractive effect since the pressure is lower between the two bodies due to the increase in flow velocity. The second is related to the vorticity produced at the surface of a body. Vorticity diffuses into the boundary layer which is formed on the body and is advected in the wake. The asymmetry induced in the vorticity field by the presence of the other body results in a repulsive force. The relative strength of the two effects depends on the Reynolds number and on the distance separating the two bodies, as discussed by Legendre, Magnaudet & Mougin (2003) in the case of two spherical bubbles, but also on the boundary condition on the body (no-slip for a solid body or shear-free for a bubble), as discussed by Takemura & Magnaudet (2003) in the twin problem of a clean or contaminated bubble interacting with a wall.

For fixed three-dimensional bodies displaying a stationary wake, substantial progress concerning the nature of the interaction between two solid spheres (Kim, Elghobashi & Sirignano 1993) and two spherical bubbles (Legendre *et al.* 2003) placed side by side has been achieved thanks to numerical simulations. For solid spheres and Reynolds numbers spanning from 50 to 150, Kim *et al.* (1993) showed the existence of a critical distance Δ_{h1} below which the spheres repel and above which they weakly attract one another up to a distance at which they have no effect on each other of about $\Delta_h \simeq 21$ (Δ_h denotes the centre-to-centre distance between the two bodies made dimensionless using their diameter d). Moreover, they showed that Δ_{h1} decreases with the Reynolds number ($\Delta_{h1} \simeq 8$ for $Re = 50$, $\Delta_{h1} \simeq 4$ for $Re = 100$ and $\Delta_{h1} \simeq 3.5$ for $Re = 150$); the range of separation distances for which the attractive potential effect is dominant over the repulsive vortical effect is extended when the Reynolds number increases. The hydrodynamical interaction between two fixed bubbles placed side by side in an incoming flow was investigated by Legendre *et al.* (2003). Below a critical Reynolds number close to 30, the bubbles repel one another. For larger Reynolds numbers, two critical distances were identified, Δ_{h1} and Δ_{h2} with $\Delta_{h1} < \Delta_{h2}$, that depend on Re ($\Delta_{h1} \simeq 1.5$ for $Re = 30$ and decreases when Re increases; $\Delta_{h2} \simeq 2$ for $Re = 30$ and increases to $\Delta_{h2} \simeq 6$ for $Re = 100$). In the interval between these two relative positions, the bubbles attract each other, outside it they repel. Note that the equilibrium distance Δ_{h1} is smaller for bubbles than for solid spheres, in line with a production of vorticity greater in the case of a no-slip boundary condition leading to a repulsive force stronger for solid spheres than for spherical bubbles at the same Re. A model for the coefficient C_L associated with the transverse force acting between two fixed bubbles was developed by Legendre *et al.* (2003). For $Re \geqslant 30$ and $\Delta_r \geqslant 3$,

$$C_L = -6\Delta_r^{-4}\left[\left(1 - \frac{40}{Re} + O(Re^{-3/2})\right) + \Delta_r^{-3} + O(Re^{-1}\Delta_r^{-2}, \Delta_r^{-5})\right] \tag{1.1}$$

where $\Delta_r = 2\,\Delta_h$ is the distance separating the centres of the bubbles normalized with their radius $d/2$. The first term, in Δ_r^{-4}, corresponds to the attractive potential effect whereas the term in $-1/Re$ corresponds to the repulsive effect of vorticity.

The case of fixed bodies placed side by side has received equal attention when the wakes of the bodies are unsteady. For a Reynolds number of 300 corresponding to unsteady wakes for solid spheres, Yoon & Yang (2007) found numerically that spheres placed side by side repel one another for all the relative distances investigated, namely $\Delta_h \leqslant 5$, indicating that repulsion between two side-by-side fixed spheres occurs for

separation distances that are larger for unsteady wakes than for steady ones. Results related to the interaction between the unsteady wakes of the bodies were also provided. Different modes of wake instability and of wake synchronization were observed depending on the distance between the bodies. In particular, Williamson (1985) investigated experimentally the wakes of two cylinders placed side by side in an incident flow with Reynolds numbers ranging from 100 to 200. For $\Delta_h > 7$, no visible interaction was observed between the wakes, whereas synchronization of vortex shedding occurred for $3 < \Delta_h < 7$. For $\Delta_h < 3$, vortices are shed at different frequencies from the two cylinders, while in the far wake they merged into a single street. Peschard & Le Gal (1996) considered the same problem theoretically and experimentally. They also reported vortex shedding either in phase or phase opposition but observed two additional regimes: first, an asymmetrical regime in which vortices are released at the same frequency but with an amplitude larger for one cylinder than for the other; and second, a quasi-periodic regime identical to the previous one but with phase and amplitude differences between the vortex shedding of the two bodies that slowly evolve in time. Schouveiler *et al.* (2004) studied numerically and experimentally the interaction of two spheres placed side by side in an incident flow at a Reynolds number of 300. They observed for $\Delta_h < 1.05$ a single wake, for $1.05 < \Delta_h < 1.3$ two asymmetrical wakes, and for $1.3 < \Delta_h < 3$ two symmetrical coupled wakes. For larger distances, the wakes appear uncorrelated in space and time.

In the case of freely moving bodies, the translational and rotational degrees of freedom of the bodies may affect the interaction and modify the hydrodynamical loads observed in the case of fixed bodies. A question also arises concerning the existence of specific modes of interaction between the wake of the bodies and their consequences on the bodies motion. Only a few studies have dealt with the interaction of freely moving solid bodies placed side by side. Wu & Manasseh (1998) studied experimentally the interaction between two side-by-side spherical particles for Reynolds numbers between 0.02 and 2000 for a fixed density ratio between the bodies and the fluid ($\rho_s/\rho_f = 1.38$). They observed that at $Re = 100$ the final distance between the particles is between 3 and 7 diameters and that their fall velocity is the same as that of an isolated particle. Synchronization of oscillatory paths was observed numerically for two-dimensional ellipsoids and for Reynolds numbers smaller than 6 by Aidun, Lu & Ding (1998) and for three-dimensional ellipsoids in a narrow channel at $Re = 100$ by Pan, Joseph & Glowinski (2005). In both studies, they found that both the inclination and the path of the two ellipsoids oscillate in phase opposition.

In this paper, we investigate the behaviour of two identical solid bodies freely falling in the side-by-side configuration, and more specifically of two axisymmetric bodies that can be viewed as finite-thickness disks. The goal of the present paper is twofold: to characterize the kinematics of the interaction of these bodies and propose an empirical model for its driving force; and to investigate if specific modes of body motion arise due to wake interaction, in particular when periodic vortex shedding occurs. The kinematics and the dynamics of finite-thickness disks were investigated in detail in the isolated body case by Fernandes *et al.* (2007) and Fernandes *et al.* (2008). These studies showed notably the strong impact of the aspect ratio of the body (the diameter-to-thickness ratio of the disk) on the characteristics of its path and on the loads governing its motion, in particular on those related to the vorticity produced at the body surface. The body geometry is therefore expected to also have an important effect on the hydrodynamical interaction between the two bodies.

The layout of the paper is the following. Section 2 presents the experimental setup used for the investigation. Section 3 focuses on the kinematics associated with the

interaction of the two disks in the case of rectilinear paths. A model for the horizontal repulsion between the bodies is then proposed in § 4. Finally, the interaction of disks displaying oscillatory paths is considered in § 5. The main results of the paper are outlined in § 6.

2. Experimental setup

The bodies are released in a large glass tank (1.70 m high with a square cross-section of 0.4 m width) containing salted water of density $\rho_f = 1010\,\mathrm{kg\,m^{-3}}$ and kinematic viscosity $\nu = 1.020\,\mathrm{mm^2\,s^{-1}}$ (see figure 1 of Fernandes *et al.* 2007). The bodies are finite-thickness disks (or short-length cylinders) of density $\rho_s \simeq 1020\,\mathrm{kg\,m^{-3}}$ (the density ratio between the bodies and the fluid is thus close to unity). Their diameters d (resp. heights h) range from 5 to 20 mm (resp. 1 to 5 mm). The aspect ratio $\chi = d/h$ is chosen at the values of 3, 6 and 10, determined with an accuracy of $\pm 1\,\%$. The motion of the body depends on the Archimedes number Ar defined by $Ar = ((\Delta\rho/\rho_f)\, g\, r_{eq})^{1/2} r_{eq}/\nu$, where $\Delta\rho = |\rho_f - \rho_s|$, r_{eq} is the radius of the sphere having a volume equal to that of the body, and g is the gravitational acceleration. Note that Ar corresponds to a Reynolds number based on a gravitational velocity. Three characteristic values of Ar are considered here, about 35, 45 and 105, allowing us to investigate both rectilinear and periodic motions (Fernandes *et al.* 2007). When the bodies are falling alone in the tank, these values of Ar correspond to the Reynolds numbers $Re = U_m\, d/\nu \simeq 110$, 140 and 280, U_m being the mean vertical velocity of the body.

In this paper, we focus on the hydrodynamical interaction between two disks that can be considered within experimental accuracy as identical. Special care was taken to select the pairs. In fact, a difference of 1 % between the mean vertical velocities of the disks (due to tiny differences in geometry or density) leads to a vertical separation of 1.5 cm at the bottom of the tank, larger than a disk diameter. Therefore only the pairs of disks for which the vertical separation distance remained smaller than a body diameter all over their paths were considered for the experiments. The two disks were released simultaneously in one or two vertical parallel tubes using a sliding plate on which the bodies rested at the time of release. A single tube or two separate tubes were used according to the size of the bodies and to the initial separation distance investigated. The release tubes enabled the bodies to accelerate while being restrained in their transverse motion and rotation. At the exit of the tubes, the bodies were falling broadside to the vertical and side by side, at a velocity close to their terminal velocity, and were free to interact. The motion of the bodies was then recorded by means of two perpendicular travelling cameras. The image- and signal-processing techniques used to determine the time evolution of the coordinates of the centre of the bodies and the angles defining the inclinations of their symmetry axes are described in detail in Fernandes *et al.* (2007). The use in this case of two PCO 2000 cameras of spatial resolution 2048×2048 pixels provided an accuracy of ± 0.06 mm for the position and of $\pm 0.75^\circ$ for the inclination. Each camera recorded the positions of the centre of gravity of the bodies in a vertical plane, denoted (X, Z) and (Y, Z), where Z is the vertical coordinate and X and Y are horizontal perpendicular coordinates. In what follows, the separation distance between the bodies is characterized by the vertical distance $\Delta_z^* = Z_1 - Z_2$ and the horizontal distance $\Delta_h^* = ((X_1 - X_2)^2 + (Y_1 - Y_2)^2)^{1/2}$, where indices 1 and 2 each stand for a body.

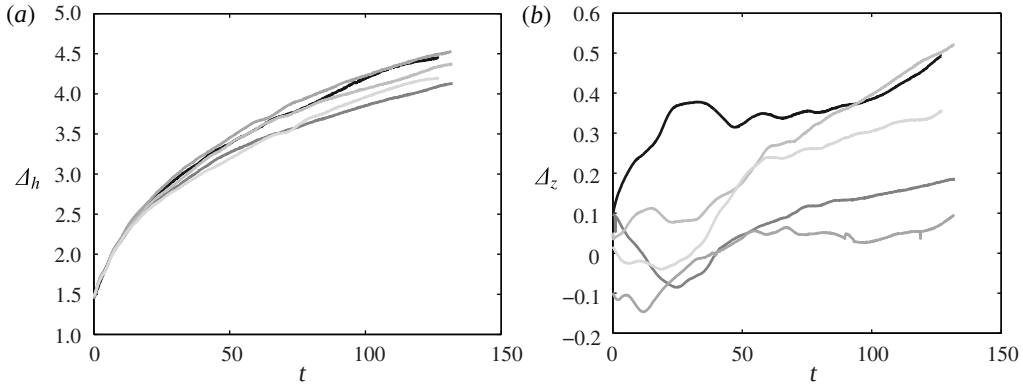

FIGURE 1. Examples of the evolution of the dimensionless (*a*) horizontal distance Δ_h and (*b*) vertical distance Δ_z between the centres of gravity of the bodies as a function of the dimensionless time $t = t^* U_m/d$ for five cases with $\chi = 10$, $Re = 115$, $d = 9\,\text{mm}$, $U_m = 13.2\,\text{mm}\,\text{s}^{-1}$.

3. Kinematics of repulsion of disks having rectilinear paths

We first consider the case of disks displaying a rectilinear path when falling alone in the tank. Along this path, the axis of symmetry of the body is aligned with the vertical. The effect of the interaction is illustrated here for disks with $\chi = 10$ but the same behaviour is observed for the aspect ratios $\chi = 3$ and 6. Figure 1(*a*) presents the evolution of the horizontal distance separating the centres of gravity of the two disks normalized with their diameter d, $\Delta_h = \Delta_h^*/d$, as a function of the dimensionless time $t = t^* U_m/d$, for $\chi = 10$ and $Re = 115$. Several cases are presented. In all these, the disks are initially very close, $\Delta_h(t = 0) < 1.5$ (and > 1 to avoid contact). The curves were repositioned at the origin to account for the differences in initial separation distances. In all cases, horizontal repulsion between the bodies occurs, which is stronger when the bodies are closer. There is however some scatter between the tests although the dimensionless parameters that control the problem are identical within experimental accuracy and the initial conditions very close. For instance, the final separation distance (at $t = 130$) spans between 4 and 4.5 diameters. This difference might be due to the fact that the bodies are not perfectly horizontally aligned during their fall. The vertical distance separating the centres of gravity of the disks normalized with their diameter d, $\Delta_z = \Delta_z^*/d$, is always less than $\Delta_z < 0.5$ but varies in time as shown in figure 1(*b*). However, no clear relationship could be established between the horizontal and vertical evolutions. Note also that the sideways motion of the disks due to the repulsion is very slight. The horizontal drift of the disks in the side-by-side situation represents about 2.5 % of their overall vertical displacement (typically 3 cm compared to 1.2 m). Fernandes *et al.* (2007) observed for isolated disks a random drift related to experimental imperfections, such as residual fluid movements or small defects in the geometry or the homogeneity of the disks, of the same order of magnitude. The clear and systematic trend observed for Δ_h seems to indicate that specific disturbances in the path of each disk do not significantly affect the repulsion effect but this may explain the scatter in the evolution of Δ_h and the irregularities observed for Δ_z. We measured that, as soon as the bodies leave the release tubes, they reach their terminal vertical velocities in a few seconds, so that the paths are performed at constant vertical velocity. As could

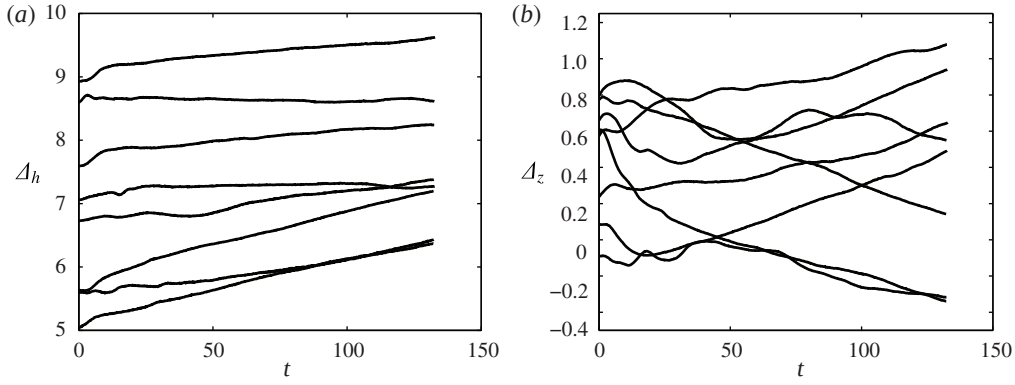

FIGURE 2. Examples of the evolution of the dimensionless (*a*) horizontal distance Δ_h and (*b*) vertical distance Δ_z between the centres of gravity of the bodies as a function of the dimensionless time $t = t^* U_m/d$ for eight cases with $\chi = 10$, $Re = 115$, $d = 9$ mm, $U_m = 13.2$ mm s^{-1}.

be expected from the weakness of the repulsion effect, the mean fall velocity U_m of the disks during the interaction is within measurement accuracy identical to those measured when the disks are falling alone.

We also explored the behaviour of the disks when the initial separation distance is larger. Typical results are shown in figure 2(*a*), for $\chi = 10$ and $Re = 115$. For a horizontal separation distance $\Delta_h > 6$, the behaviours of the disks appear as decoupled. For these distances, the interaction effect between the disks is of the same order of magnitude as the disturbances present in the trajectory of each disk, so that the three behaviours, attraction, repulsion and indifference, can be observed, either consecutively along the same path or for different trials with the same bodies. We carried out a large number of trials for separations close to this distance, approximately 15 per aspect ratio, in order to determine the limit below which a significant interaction effect can be observed, i.e. a reproducible effect that is stronger than the background experimental noise. We obtained that for all χ, when $\Delta_h < 4.5$, the disks always repel each other; for $\Delta_h < 6$, they never come closer and for $\Delta_h > 6$ no significant interaction seems to occur between the disks.

We now focus our attention on the effect of the aspect ratio on the repulsion effect observed for disks falling sufficiently close together. Figure 3(*a*) presents the evolution of the horizontal distance Δ_h as a function of time for the aspect ratios $\chi = 3$, 6 and 10 and for $Re = 115 \pm 10$, and figure 3(*b*) the corresponding evolution of Δ_z. Seven cases are shown revealing, rather surprisingly, the same evolution for thin and thick bodies. The scatter of the results between the different aspect ratios is of the same order of magnitude as the scatter of the results for one aspect ratio so that the kinematics of repulsion can be considered in a first approximation as independent of the aspect ratio (and therefore of the body thickness). For all χ and $\Delta_h \geqslant 1.5$, the mean evolution of the set of curves displayed in figure 3(*a*) can be fitted by the power law shown with a dashed red line, which is

$$\Delta_h \sim a\, t^b \quad \text{with } a = 1.1 \text{ and } b = \frac{2}{7}. \tag{3.1}$$

The upper and lower limit of the set of curves can then be obtained by varying a by $\pm 2.5\,\%$ or b by $\pm 1.5\,\%$.

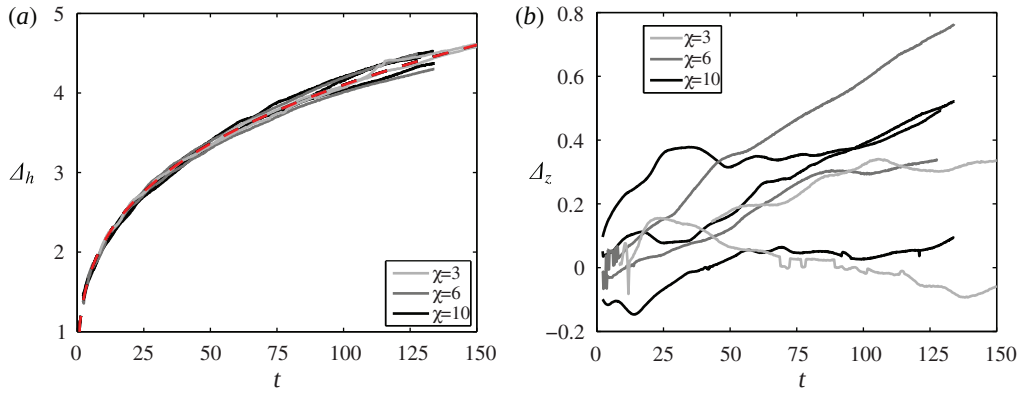

FIGURE 3. Dimensionless (a) horizontal distance Δ_h and (b) vertical distance Δ_z between the centres of gravity of the bodies as a function of the dimensionless time t: two cases for $\chi = 3$, $Re = 105$, $d = 5.7$ mm, $U_m = 18.8$ mm s^{-1}; two cases for $\chi = 6$, $Re = 125$, $d = 7.2$ mm, $U_m = 14.9$ mm s^{-1}; three cases for $\chi = 10$, $Re = 115$, $d = 9$ mm, $U_m = 13.2$ mm s^{-1}. The dashed red line corresponds to (3.1).

4. A model for the repulsion between two disks falling side by side

The aim of this section is to model the repulsive force on each disk that leads to the kinematics determined in the previous section. Following the approach of Takemura & Magnaudet (2003) for a bubble interacting with a fixed wall, we consider that within a quasi-steady hypothesis a transverse drag force balances the repulsion force related to the modification of the flow about the body induced by the other body. For rectilinear paths of the bodies, the transverse drag force can be estimated from the results for a fixed body placed with a given incidence angle in a uniform flow. Fernandes (2005) determined by numerical simulations the force acting on a fixed disk of aspect ratio χ placed with different angles of attack in a uniform flow. He showed that the transverse drag force (i.e. the component of the force along the transverse direction y of the body) can be written as a classical drag force, i.e. as the product between the norm U^* of the velocity of the disk, the transverse velocity v^* and a dimensionless coefficient C_y that depends on the aspect ratio of the body. For $2 \leqslant \chi \leqslant 10$, the numerical values obtained for C_y can be conveniently modelled by $C_y = 2/\chi$. Denoting as F_r the repulsion force induced by the interaction and as C_r the dimensionless repulsion force coefficient such that $F_r = C_r \rho_f S_{ref} U^{*2}/2$, the quasi-steady force balance in the transverse direction of a disk is then

$$\tfrac{1}{2} C_r \rho_f S_{ref} U^{*2} = \tfrac{1}{2} C_y \rho_f S_{ref} U^* v^* \tag{4.1}$$

where $S_{ref} = \pi d^2/4$. This equation becomes, in non-dimensional form, $C_r = 2v/\chi$, where $v = v^*/U^*$ is the dimensionless transverse velocity. Note that at leading order U^* is close to the mean fall velocity U_m of the body, so that U_m will be applied in the following. We now use (3.1), characterizing the experimental kinematics of repulsion of the two bodies, to obtain the power-law dependence of the transverse velocity v and of C_r on the horizontal distance Δ_h. For each disk, we have

$$v = \frac{1}{2}\frac{\mathrm{d}\Delta_h}{\mathrm{d}t} = \frac{a}{2} b t^{(b-1)} = \frac{1}{2} a^{1/b} b \Delta_h{}^{(b-1)/b} \tag{4.2}$$

so that we get for the repulsion coefficient

$$C_r = \frac{1}{\chi} a^{1/b} b \Delta_h^{(b-1)/b}. \tag{4.3}$$

Using the experimental values $a = 1.1$ and $b = 2/7$ leads to

$$C_r \simeq 0.4 \frac{1}{\chi} \Delta_h^{-5/2} \quad \text{for } 1.5 < \Delta_h < 5. \tag{4.4}$$

Equation (4.4) indicates that the repulsive force acting between two identical disks falling side by side is inversely proportional to their aspect ratio (it varies as $1/\chi$) and decreases with their separation distance as $\Delta_h^{-5/2}$. In the case of spherical bubbles, the repulsive force coefficient decreases more rapidly as Δ_h^{-4}. This difference is in line with a production of vorticity that is stronger for solid disks than for bubbles. Finally, note that the χ^{-1} dependence of the repulsion coefficient C_r thus being stronger for thicker bodies, leads to the kinematics of repulsion that is independent of the aspect ratio observed in figure 3(*a*).

5. Interaction of two bodies having periodic paths

Above a critical Reynolds number that depends on the aspect ratio, the bodies display a quasi-planar zigzag motion, their velocity and orientation oscillate and periodic vortex shedding occurs in the wake of the bodies (Fernandes *et al.* 2007). For these periodic paths, we observed that the predominant effect of the interaction for two bodies falling side by side is repulsion, as also happens in the case of rectilinear paths. Figure 4(*a*) presents the evolution of the horizontal distance Δ_h between the centres of gravity of the bodies as a function of the dimensionless time t for $Re \approx 280 \pm 5$ and figure 4(*b*) the corresponding vertical separation distance. For readability, only two cases are plotted. Since the disks do not oscillate in phase, both horizontal and vertical separation distances oscillate. The scatter of the results for Δ_h is larger than in the case of rectilinear paths. For instance the relative distance Δ_h varies between 3 and 3.8 at the dimensionless time $t = 70$. The envelope containing the mean evolution of Δ_h for all tests is plotted with dashed lines in figure 4(*a*). The two limit curves evolve as in the case of the rectilinear paths as $\Delta_h = at^b$ with $b = 2/7$ for $\Delta_h \geqslant 1.5$. The factor a is equal to 0.9 for the lower limit and 1.1 for the upper limit. This upper limit corresponds to the case where the repulsion velocity is the most important and is identical to the expression obtained for disks with rectilinear trajectories (3.1). Oscillating disks therefore repel each other slightly slower than disks having rectilinear motion, and expression (4.3) remains a good approximation for the repulsion coefficient driving the sideways motion on a timescale much longer than the period of oscillation of the bodies.

We observed that the characteristics of the oscillatory motion of the disks are unaffected by the side-by-side repulsion: within experimental accuracy, the mean fall velocity U_m, the Strouhal number and the amplitudes of oscillation in position and inclination are unchanged compared to those measured for isolated disks (Fernandes *et al.* 2007). The eventuality of synchronization of the motion of the bodies due to synchronization of the vortex shedding in their wakes was also carefully investigated. As mentioned in the introduction, vortex shedding for two fixed bodies may synchronize. For objects in free fall investigated numerically in a two-dimensional geometry by Aidun *et al.* (1998) and in a confined geometry by

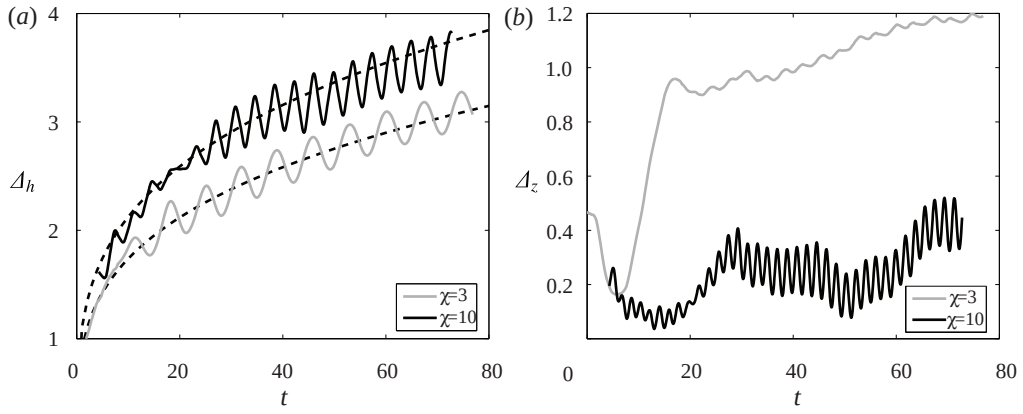

FIGURE 4. Dimensionless (*a*) horizontal distance Δ_h and (*b*) vertical distance Δ_z between the centres of gravity as a function of the dimensionless time for oscillating disks: $\chi = 3$, $Re = 285$, $d = 12$ mm, $U_m = 23.9$ mm s^{-1}; $\chi = 10$, $Re = 275$, $d = 18$ mm, $U_m = 15.4$ mm s^{-1}. Dashed lines in (*a*): (3.1) with $a = 0.9$ (lower line) and $a = 1.1$ (upper line), $b = 2/7$.

Pan *et al.* (2005) synchronization was also observed leading to oscillations of the trajectory and of the inclination of the bodies in phase or in phase opposition. In our case, despite extensive investigation, phase synchronization of the oscillations of the two disks was not observed. This may be due to the fact that in the case of freely falling bodies in a three-dimensional configuration, additional degrees of freedom influence the interaction between the wakes of the bodies and cause the absence of phase-locking between the paths of the two disks. In particular, in the three-dimensional configuration, the vertical planes containing the paths of the two bodies are generally distinct, they depend on initial conditions and may rotate slightly, as happens in the case of isolated bodies (Fernandes *et al.* 2007).

6. Conclusion

This paper is devoted to the hydrodynamical interaction of two identical freely falling disks placed side by side for Reynolds numbers ranging from 100 to 300, corresponding to rectilinear and oscillatory paths. Careful experiments allowed us to bring to light a weak, though clear and systematic, repulsion effect between the disks for the three aspect ratios investigated. For bodies initially nearly in contact, this effect typically leads to a sideways motion of the body of about 2 diameters for a vertical displacement of 120 diameters. We observed that the disks always repel one another when the horizontal distance between their centres of gravity is less than 4.5 diameters. They never come closer for distances between 4.5 and 6 diameters. For distances greater than 6 diameters, the disks appear to have no effect on each other. For disks displaying rectilinear paths, we present a model for the repulsion coefficient C_r, which decreases with the separation distance between the bodies and is inversely proportional to their aspect ratio, varying like $1/\chi$, so that the coefficient is stronger for thicker bodies. The proposed model satisfactorily reproduces the kinematics of interaction observed experimentally. Though we did not determine the dependence of C_r on the Reynolds number, it appears that for the oscillatory paths the strength of the repulsion effect decreases slightly, being at most 20 % lower at $Re = 300$ than at $Re = 100$, whatever χ. However, for the oscillatory paths, the most notable

result is that no synchronization is observed between the paths and between the wakes of the two disks, and that the only apparent effect of the interaction is the weak horizontal repulsion occurring until the bodies reach the distance at which they have no detectable effect on each other of about 6 diameters. Our three-dimensional experiments indicate that the degrees of freedom of the bodies are able to inhibit the synchronization phenomenon observed for fixed bodies or in constrained geometries for freely moving bodies. It is also noteworthy that the characteristics of the oscillatory motion of each disk appear unaffected by the interaction, indicating that in the range of parameters investigated the dynamics of the oscillatory motion of a disk are robust with respect to the flow generated by the presence of an identical disk at its side.

Acknowledgements

The authors are grateful to Hervé Ayroles, Sébastien Cazin and Gregory Ehses for the technical support provided for the experiments.

References

AIDUN, C. K., LU, Y. & DING, E. J. 1998 Direct analysis of particulate suspensions with inertia using the discrete Boltzmann equation. *J. Fluid Mech.* **373**, 287–311.

FERNANDES, P. C. 2005 Etude expérimentale de la dynamique de corps mobiles en ascension dans un fluide peu visqueux. PhD thesis, Institut National Polytechnique de Toulouse.

FERNANDES, P. C., ERN, P., RISSO, F. & MAGNAUDET, J. 2008 Dynamics of axisymmetric bodies rising along a zigzag path. *J. Fluid Mech.* **606**, 209–223.

FERNANDES, P. C., RISSO, F., ERN, P. & MAGNAUDET, J. 2007 Oscillatory motion and wake instability of freely rising axisymmetric bodies. *J. Fluid Mech.* **573**, 479–502.

KIM, I., ELGHOBASHI, S. & SIRIGNANO, W. A. 1993 Three-dimensional flow over two spheres placed side by side. *J. Fluid Mech.* **246**, 465–488.

LEGENDRE, D., MAGNAUDET, J. & MOUGIN, G. 2003 Hydrodynamic interactions between two spherical bubbles rising side by side in a viscous liquid. *J. Fluid Mech.* **497**, 133–166.

PAN, T. W., JOSEPH, D. D. & GLOWINSKI, R. 2005 Simulating the dynamics of fluid-ellipsoid interactions. *Comput. Struct.* **83** (6-7), 463–478.

PESCHARD, I. & LE GAL, P. 1996 Coupled wakes of cylinders. *Phys. Rev. Lett.* **77** (15), 3122–3125.

SCHOUVEILER, L., BRYDON, A., LEWEKE, T. & THOMPSON, M. C. 2004 Interactions of the wakes of two spheres placed side by side. *Eur. J. Mech. B/Fluids* **23** (1), 137–145.

TAKEMURA, F. & MAGNAUDET, J. 2003 The transverse force on clean and contaminated bubbles rising near a vertical wall at moderate Reynolds number. *J. Fluid Mech.* **495**, 235–253.

WILLIAMSON, C. H. K. 1985 Evolution of a single wake behind a pair of bluff bodies. *J. Fluid Mech.* **159**, 1–18.

WU, J. & MANASSEH, R. 1998 Dynamics of dual-particles settling under gravity. *Intl J. Multiphase Flow* **24** (8), 1343–1358.

YOON, D.-H. & YANG, K.-S. 2007 Flow-induced forces on two nearby spheres. *Phys. Fluids* **19** (9), 098103.